FINITE ELEMENT AND ANN-BASED PREDICTION OF BEARING CAPACITY OF SQUARE FOOTING RESTING ON THE CREST OF *c-φ* SOIL SLOPE

R. Acharyya

Research Scholar, Department of Civil Engineering, Indian Institute of Technology Guwahati, Assam, India.

Email: r.acharyya@iitg.ernet.in

A. Dey

Assistant Professor, Department of Civil Engineering, Indian Institute of Technology Guwahati, Assam, India.

Email: arindamdeyiitg16@gmail.com

B. Kumar

Associate Professor, Department of Civil Engineering, Indian Institute of Technology Guwahati, Assam, India.

Email: bimk@iitg.ernet.in

ABSTRACT

For footings located on or near a slope, the slope face acts as a finite boundary that leads to an inadequate development of the resisting passive zone. Depending upon the footing location and slope inclination, the outward deformation of the soil from beneath the loaded footing might lead to substantial reduction in the bearing capacity. A series of finite element analysis has been carried out using Plaxis 3D vAE.01 to investigate the bearing capacity of a square footing placed on crest of the slope. The effect of various geotechnical and geometrical parameters of the footing has also been investigated. Based on the simulated outcomes, an optimal 7-10-1 artificial neural network (ANN) architecture has been developed for the direct prediction of bearing capacity based on the input parameters. Sensitivity analysis conducted using Garson's algorithm and Connection-weight approach revealed that angle of internal friction of the slope constituent material and the embedment depth have the highest importance ranking.

Keywords: *Ultimate bearing capacity, Footings on slope, Square footing, Finite element, ANN*

1.0 INTRODUCTION

Bearing capacity of foundations is one of the prime concerns for geotechnical engineers as it aids in its assessment and design. Design of foundations on a horizontal ground surface depends on the mechanical characteristics of the soil (unit weight and shear strength parameters) and the physical properties of the foundation (depth, width, and shape of the footing). There are two primary considerations to decide the allowable bearing pressures of shallow foundations: (a) the safety factor against ultimate shear failure must be adequate, and (b) the settlements should not exceed the acceptable limits. Conventionally, the ultimate bearing capacity of foundation is defined as the maximum stress that it can carry without undergoing a shear failure. Based on the shear strength parameters of the soil, Terzaghi (1943) was the first to quantify the ultimate bearing capacity of a strip footing resting on a uniform horizontal ground, which is used extensively even today. The basic proposition for the bearing capacity of strip footings has undergone several modifications, primarily related to the theoretical bearing capacity factors, as well as inclusion of several new contributory factors (Meyerhof 1951; Vesic 1973; Hansen 1970). However, strip footings are not commonly used as building foundations, except for the load bearing walls. Hence, in order to accommodate different shapes of the footings (square, rectangular, circular or combined), shape factors were introduced in the bearing capacity expressions (Vesic 1973; Hansen 1970).

Rapid growth of urbanization in the North-Eastern hilly regions of India has resulted in myriads of residential and commercial constructions. The foundations of such constructions are mostly shallow, and are located either on the crest or on the benched face of the slopes. Apart from the urban constructions, transmission towers, water tanks, retaining walls, footings for bridge abutments, and even foundations for transportation links are mostly located on the slopes. Foundation on slopes is a challenging and complex problem for the geotechnical engineers. The stability of a footing on or near a slope is affected by its location, the loading characteristics, the edge distance from the slope face (i.e. setback distance), the slope angle, the depth of embedment of the footing, the shear strength characteristics of the foundation soil, and other additional factors, such as the rainfall, seismicity and saturation level of the foundation material. For footing placed near to face of a slope, a reduction in the bearing capacity of the foundation is expected due to the curtailed zone of passive resistance developed towards the slope face.

It is observed that in contrast to the footings resting on horizontal ground (Zhu and Michalowski 2005; Cerato and Lutenegger 2006; Cerato and Lutenegger 2007; Yu et al. 2010; Lavasan and Ghazavi 2014), there

exists limited reports on experimental investigations related to the estimation of the bearing capacity of a footing located on a slope (Shields et al. 1977; Bauer et al. 1981; Kumar and Ilamparuthi 2009; Castelli and Lentini 2012; Azzam and Farouk 2010; Keskin and Laman 2013; Acharyya and Dey 2017; Azzam and El-Wakil 2015; Shukla and Jakka 2017). Most of the attempts have been made to evaluate the bearing capacity of a strip footing, resting on dry cohesionless sandy soil slope, and to investigate the effects of the governing parameters (setback distance, width of the footing, relative density of slope material, steepness of the slope and type of loading on the footing). Very few literatures exist related to the laboratory or numerical investigations of square and circular footings resting on a slope (Castelli and Lentini 2012; Shukla and Jakka 2017; Acharyya and Dey 2017).

Neural networks, as they are identified today, initiated from the research of McCulloch and Pitts (1943), who established the capability of interconnected neurons to calculate some logical functions. Hebb (2002) reported in detail the importance of the synaptic connections in the learning process. Later, Rosenblatt (1958) offered the first operational model of a neural network: the 'Perceptron'. The perceptron, built as an analogy to the visual system, was able to learn logical functions by modifying the synaptic connections. Artificial neural networks (ANNs) are usually employed when the relationship between the input and output is complicated, or when the application of another available method becomes computationally expensive.

Many researchers in different fields of the civil engineering have recently used ANN architectures. Lee and Lee (1996), Das and Basudhar (2006) and Momeni et al. (2008) used ANN for forecasting the pile bearing capacity. Ghaboussi, Sidarta, and Lade (1994) showed that ANNs are powerful tools for the mathematical constitutive modelling of geomaterials. Shahin, Maier, and Jaksa (2002) successfully applied back propagation Multi-Layer Perceptron's (MLPs) to predict settlement of shallow foundations on granular soils. Goh (1994) demonstrated that ANNs could model the complex relationship between seismic soil parameters and liquefaction potential using actual field records. The prediction of swelling pressure and hydraulic conductivity characteristics of clayey soil has been investigated by several researchers (Erzin et al. 2009; Das et al. 2010; Das, Samui, and Sabat 2012; Mishra, Kumar, and Dutta 2016). Noorzaei, Hakim, and Jaafar (2008), Kuo et al. (2009), Behera et al. (2013I, 2013II) used ANNs for predicting the ultimate bearing capacity of strip footing resting on horizontal ground surface subjected to centric and eccentric loading.

Habitats in the hilly regions mostly comprise of the houses resting either on the slope face or on the crest. A 'Compilation of the catalogue of the building typologies in India' revealed that most of the buildings

located in the hilly terrains in the North-Eastern regions of India are supported by shallow isolated footings (NDMA 2013). Hence, it is important to address and understand the mechanism of failures of shallow isolated square footings resting on the *c*-φ soil-slope. However, very limited literature exists in this regard. Castelli and Lentini (2012) and Acharyya and Dey (2017) reported experimental and numerical studies for a square footing placed on the crest of a dry sandy slope, solely to study the effect of various geotechnical and geometrical parameters on its ultimate bearing capacity and the associated bearing capacity factor. It has been observed that, for real case scenario, the hill-slopes are made of *c*-φ material. Hence, based on 3-D finite element (FE) simulations using Plaxis 3D vAE.01, this article reports the effect of various geotechnical and geometrical parameters on the ultimate bearing capacity of a square footing resting on crest of *c*-φ soil-slopes. The 3D numerical model also provides a description of the failure mechanism involved in the process of loading and failure of the footing. From the outcomes of the parametric investigation, an artificial neural network (ANN) based model has been developed for the prediction of ultimate bearing capacity (q_u) of square footing resting on crest of *c*-φ soil-slope. From the ANN results, a sensitivity analysis has been performed to realize the prominence of various geotechnical and geometrical parameters used for assessing ultimate bearing capacity.

2.0 PLAXIS 3D FINITE ELEMENT ANALYSIS

Plaxis 3D vAE.01 is a finite element (FE) package intended for three-dimensional analysis of deformation, stability and ground water flow in geotechnical engineering. Plaxis 3D is equipped with several features to deal with various aspects of complex geotechnical problems incorporating advanced constitutive models for simulations of non-linear, time-dependent and anisotropic behaviour of soil or rock. It has been observed from the past research (Castelli and Lentini 2012; Acharyya and Dey 2017) that dry cohesionless soil-slope has been taken into account for investigation of the bearing capacity of square footing resting on or near the slope. However, in real situation, the hill-slopes are made of different types of soils, ranging from fine silts, marginal soil mixtures, gravels, as well as highly weathered rock masses. As a result, finite element 3-D analysis has been carried out to study the behaviour of a shallow square footing resting on a generalized *c*-φ soil slope, with an aim to represent the commonly occurring building foundations in the hill slopes of North-Eastern India.

2.1 Description of the Modelling

Figure 1 shows the schematic diagram of a footing resting on the crest of a slope. In accordance to Boussinesq's elastic stress theory, the "$0.1q$" stress contour (q is the stress applied on the footing up to its failure) represents the significant isobar, beyond which the effect of the applied stress is considered to be negligible. The model dimensions have been so chosen that the significant isobar is not intersected by the model boundaries (Figure 1). In the numerical model, "standard fixity" condition has been employed. Horizontal fixity was applied to the lateral vertical edges, while the bottom edge of the model is assumed to be non-yielding and restrained from both vertical and horizontal movements (Figure 2). The inclined slope face is devoid of any fixity, allowing for free deformation occurring due to the location and loading of the footing. In order to estimate the bearing capacity of footing in the numerical framework, various locations of a square footing have been chosen for the numerical analyses. Figure 3 shows the different locations of the surface and embedded footings on the crest or the face of the sloping ground.

To perform the finite element analysis, the model geometry is discretized into smaller finite number of elements. For the Plaxis 3D finite element mesh, the basic soil elements are the 10 noded tetrahedral elements, as shown in Figure 2. Plaxis 3D program allows for a fully automatic generation of finite element meshes. In Plaxis 3D, five basic meshing schemes are available, namely 'Very coarse', 'Coarse', 'Medium', 'Fine', and 'Very fine', governed by their associated 'Mesh coarseness factor'. The mesh should be sufficiently and optimally fine to obtain accurate numerical results. A very coarse mesh fails to capture the important characteristic responses of the domain. Beyond optimally fine meshes, there are chances of the accumulation of numerical errors, thereby producing inaccuracy in the obtained information. Moreover, very fine meshing should be avoided since it will take excessive time for calculations, and in many cases, without resulting in sufficient enhancement in the preciseness of the results. Any basic meshing scheme can be adopted, with further provisions of local refinements, as demanded by the merit of the problem and the location of the response points in the numerical simulation.

For the present study, the soil is modelled by linear elastic-perfectly plastic Mohr-Coulomb (M-C) model which involves five input parameters, i.e. elastic parameters (stiffness E and Poisson's ratio ν) and strength parameter (soil plasticity parameters: φ, angle of internal friction, and c, cohesion; dilatancy parameters: ψ, angle of dilatancy). Plasticity theory specifies that, if the dilatancy angle is not identical to the friction angle, the material follows a non-associated flow rule. The dilatancy angle varies from zero to the soil

friction angle. Correspondingly, dilative coefficient, η, relates the dilatancy angle to the soil friction angle, and is defined as $\eta = \psi / \varphi$. Theoretically, the magnitude of dilative coefficient lies in the range $0 \le \eta \le 1$. The case η =1 directs that the material follows an associated flow rule (Drescher and Detournay 1993; Xiao-Li et al. 2007). In the present investigation, associated flow rule has been taken into account, and hence, for each value of friction angle φ, dilation angle ψ has been considered equal to φ. The variations of geotechnical and geometrical parameters used in the present study are given in Figure 4.

The rigid square footing, with a rough base and thickness 0.2 m, has been modelled with 10 noded tetrahedral element , formed with M20 concrete material, was represented by using linearly elastic model and the parameters are tabulated in Table 1. An interface element is provided at the boundary of the concrete and soil elements, the stiffness matrix of which was obtained using Newton-Cotes integration points (Nasr 2014). The interface parameters were simulated by assigning a suitable value to the interface strength reduction factor (R_{inter}), which controls the soil strength mobilized at the interface during the deformation. For the present study, the strength reduction factor for the soil-concrete interface was assigned to be 1 (one), thus allowing no relative movement between the footing and the soil; hence, the footing is modelled as rough strip footing.

3.0 ARTIFICIAL NEURAL NETWORK MODELLING

Neural networks are data processing systems consisting of a large number of simple, highly interconnected processing elements (artificial neurons) in an architecture inspired by the structure of the central cortex of the brain. They operate as powerful tools to capture and learn significant structures in the datasets. Neural networks can generate meaningful mapping even when the data to be processed is adulterated with incompleteness, and can process information extremely rapidly when applied to solve real world problems.

A commercial Microsoft Windows-based ANN software, Matlab v2015A (MathWorks 2001) was used for the study. This software allows the user to select the number of hidden layers, number of hidden layer nodes (neurons), iterations used during the model training, learning algorithms and transfer functions. A multilayer feed-forward cum back-propagation network, which was created by generalizing the Levenberg-Marquardt's (Mishra et al. 2006) learning rule to multiple layer networks and nonlinear differential transfer functions, was used in the present modelling. In the present study, the network architecture consists of an input layer with 10 neurons, an output layer with 1 neuron, and a hidden layer (Figure 5). The number of hidden nodes in a network

is critical to network performance. Too few nodes can lead to under-fitting, while too many nodes can lead the system toward memorizing the patterns in the data or learn noise (Das and Basudhar 2006). The transfer function used in the model is tan-sigmoid for both inputs-to-hidden and hidden-to-output layers. The idea behind choosing sigmoid functions is that it bears a greater resemblance to the biological neurons. In case of sigmoid functions, the output of the neurons varies continuously and non-linearly with the input. The maximum epochs has been set to 10000. The Mean Square Error (MSE), which specifies the error generated while learning, can be calculated using Eq. 1.

$$MSE = \frac{1}{N_d}\sum_{i=1}^{N}(O_{Simulation} - O_{ANN}) \quad (1)$$

where, N_d is the total number of data, $O_{Simulation}$ is the numerically simulated values of any entity, and O_{ANN} is the predicted values of the same entity.

4.0 STAGES OF ANALYSIS

Based on the developed 3D simulation models, several analyses have been conducted in order to explore the following:

- Validation of the numerical model
- Convergence study to determine the optimum mesh configuration
- Effect of the variation of geotechnical and geometrical parameters on the ultimate bearing capacity
- Development of ANN-based model for prediction of ultimate bearing capacity (q_u)
- Recognition of the importance ranking of the geotechnical and geometrical parameters

5.0 VALIDATION STUDY

Castelli and Lentini (2012) experimentally investigated the effect of the bearing capacity of shallow footings on slopes. The investigation had been performed with square footings of width 6 cm, 8 cm and 10 cm, resting on the sandy slope inside a model tank of dimension 100 cm long, 45 cm wide and 40 cm high. Three setback distances have been used during the experiment (b = 0.04 m, 0.12 m, 0.21 m). Load was applied incrementally by a hydraulic jack and was maintained manually with a hand pump. The vertical displacements were measured by means of displacement transducers. Settlement data were recorded using a data acquisition system having a

precision of 0.025 mm. All the tests were performed on specimens of Playa Catania (Italy) sand. A series of standard drained shear tests were carried out to evaluate the internal friction angle of the model sand using specimens prepared by dry tamping. The internal friction angle (φ) of the sand, at a relative density of 87%, was estimated approximately to be 38°, and the maximum dry density (γ_{dmax}) was obtained to be 17.50 kN/m^3. The test soil bed was constructed in layers, forming a slope angle of 30° at the face.

A 3D FE numerical model is developed to represent the experimental work reported by Castelli and Lentini (2012). In order to identify the optimal meshing configuration for the numerical model, a convergence study had been carried out (considering different footing locations and sizes) using the standard meshing schemes described earlier. The schemes are represented by their non-dimensional average element length, which is defined as the ratio of the average element length to the largest geometrical dimension of the model. Figure 6 represents the result of the convergence study for a typical footing location (b = 0.04 m), and exhibits that beyond a fine mesh, the obtained results are nearly identical. Similar results have been obtained for other configurations as well; however, those are not presented here for the sake of brevity. Based on the observations, the fine mesh (non-dimensional average element length approximately 0.086) is considered to be optimum.

In order to validate the numerical model considering the optimal mesh size, various geometrical configurations related to the footing location and setback distances have been considered for the study. The model dimensions and the material properties have been adopted identical to that of the experimental model considered by Castelli and Lentini (2012). As the stiffness parameters for the experimental model was not explicitly specified in the literature, the magnitudes of the modulus of elasticity (E_s = 15 MPa) and Poisson's ratio (v = 0.3) has been chosen in accordance to the standard references (Keskin and Laman 2013; Naderi and Hataf 2014). Figure 7 represents the comparison of the load-settlement behaviour for a typical geometrical configuration (B = 0.08 m, b = 0.12 m). A good agreement between the experimental and numerical results can be observed, thus indicating the suitability of the developed numerical model for representing the response of such foundations.

6.0 RESULTS AND DISCUSSION

6.1 Parametric Study

For footing resting on a sloping ground, the setback distance is perceived as one of the most important governing parameter in the assessment of bearing and deformation characteristics of the footing. The lesser the

setback distance, higher is the possibility of failure of the footing, exhibiting conditions of distress due to the deformation of the slope face. Hence, in order to highlight the effect of various parameters, a detailed parametric study has been conducted, keeping the setback distance as one of the contributing parameters of the simulation. For a footing resting on a sloping ground, different setback ratios were considered in the analysis, namely b/B = 0-10, and the same is represented in Figure 3.

The numerical simulation of footings resting on sloping ground, with various setback ratios (b/B), slope angles (β), footing widths (B) and embedment ratios (D_f/B) had been checked for mesh convergence, the results of which are illustrated in Figure 8. As observed earlier, fine mesh (average non-dimensional mesh size of nearly 0.18) proves to be the optimal, and hence, all the further studies for the sloping ground have been carried out with the mesh configuration. The non-dimensional mesh size is estimated in terms of the height of the model (6 m), the only parameter which remains invariant for all the simulation scenarios.

6.1.1 Influence of cohesion (c)

The influence of cohesion (c) on the ultimate bearing capacity (q_u) is exhibited in Figure 9. As obvious, higher values of cohesion resulted in higher shear strength, and hence, higher bearing capacity of the foundation. Moreover, it is noted that for any chosen value of cohesion, the bearing capacity increases up to setback ratio 4, and further exhibits an asymptotic response.

6.1.2 Influence of angle of internal friction (φ)

Figure 10 demonstrates the effect of variation of angle of internal friction (φ) on the ultimate bearing capacity (q_u). An increase in angle of internal friction involves increased inter-particle frictional contact, thus enhancing the shear strength of foundation soil, which in turn, increases the ultimate bearing capacity of the footing. In this case as well, the effect of varying setback distance remains prominent till a b/B = 2-4.

6.1.3 Influence of unit weight of soil (γ)

Four different unit weight of the soil has been chosen for the parametric study, namely γ = 12 kN/m^3, 15 kN/m^3, 17 kN/m^3 and 21 kN/m^3. Figure 11 exhibits that the variation of unit weight has negligible effect on the ultimate bearing capacity of the footing.

6.1.4 Influence of footing width (*B*)

Three different footing widths have been selected, namely B = 0.5 m, 1 m and 2 m. A larger footing width involves a larger soil domain to support the incumbent load, and the same is reflected in Figure 12 which shows a higher ultimate bearing capacity for larger footing widths.

6.1.5 Influence of slope angle (β)

Change in the slope angle (β) can significantly alter the stability conditions and bearing capacity characteristics of the footing resting on the sloping ground. A footing exhibits a higher bearing capacity while resting on or near a slope having lesser inclination. Moreover, the natural stability of the slope is governed by the slope angle in relation to the shear strength parameters of the constituent material. For the present study, four different slope angles have been considered namely β = 10°, 20°, 30° and 40°. It can be observed from Figure 13 that q_u decreases with the increase in the slope inclination. This is attributed to the fact that steeper is the slope, the zone of outward passive resistance beneath the footing will be smaller and, hence, will offer less resistance towards outward soil movement and easily succumb to failure.

6.1.6 Influence of embedment ratio (D_f/B)

Three different embedment ratios (0, 0.5, and 1) were chosen for footing resting on the crest of a sloping ground. The embedment ratio was restricted to 1, so that the footings can be considered to behave as shallow footings. Figure 14 shows that the ultimate bearing capacity (q_u) increases with the increase in the embedment ratio of footing (D_f/B), attributed to the higher confinement effect restricting the soil movement. The effect is more prominent when the footing is located away from the face of the slope due to reduced influence of the slope face.

6.1.7 Influence of setback distance (b/B)

Based on all the variations as exhibited in Figures 9-14, it can be correctly noted that beyond a setback distance of 4, the variations are nearly asymptotic, thereby indicating least influence of the slope face on the soil movement beneath the loaded footing. Hence, b/B = 4 can be conclusively stated to the limiting or critical, beyond which the response of a loaded footing will be the same as obtained when it rests in homogeneous semi-infinite medium.

For footings positioned at various locations on the crest, Figure 15 portrays the influence of setback distance of the development of the resisting mechanisms beneath a loaded footing. It can be observed that the outward passive zone (towards the slope face) is substantially affected by the nearness of the footing to the slope face. Lesser is the setback distance, lesser is the resistance offered by the passive zone since it gets largely intersected by the slope face, leading to the reduction in the bearing capacity. It has been witnessed that for a footing placed at the crest of the slope ($b/B = 0$), the formation of passive zone is largely one-directional, due to the predominant free deformation of the soil towards the slope face due to the load applied on the footing. This phenomenon results in a considerable decrease of the confinement pressure, and hence, lessening of the bearing capacity. As the setback ratio increases, the influencing effect of the slope face on the development of the passive mechanism gradually reduces. It is noted that beyond a critical setback ratio $(b/B)_{critical}$ of 4, the developed stress contours for the passive zone remains unaffected from the influence of the slope face, as if the footing is resting on a semi-infinite horizontal medium.

6.2 Results from ANN models

6.2.1 Influence of number of neurons in hidden layer

In the present investigation, a convergence study has been conducted for ascertaining the optimum number of neurons required in the hidden layer. The number of neurons in the hidden layer is varied, and as shown in Figure 16, the mean square error (MSE) achieves a minimum (0.0126) with the application of ten neurons in the hidden layer. Hence, the 7–10–1 ANN architecture is considered to be the 'best model' for the present study, containing seven (7) input nodes (c, φ, γ, B, b/B, β and D_f/B), ten (10) hidden-layer neurons, and a single (1) output node (q_u); the same is portrayed in Figure 5.

6.2.2 Training, testing and validation of the ANN architecture

A neural computing system can adjust its behaviour in response to its environment. When sets of inputs are provided to the network, it will self-adjust to produce reliable mapping through a process called training, wherein the neural (or, connection) weights methodically altered to attain the desired results. The aim of training is to find a set of connection weights that will achieve the minimum MSE in the shortest possible time (Hagan, Demuth and Beale 1996). In this regard, 80% of the total data are used for training, and the remaining 20% are

used for validation of the ANN architecture. The training dataset is further divided, where 70% of the data is used for actual training of the architecture, while the remaining 30% is used as the testing set (Ghaboussi et al. 1994). In the training process, the connection weights constantly adjusted to minimize the error between the predicted and the desired outputs. When the training gets complete, the achieved weights are maintained for the subsequent testing and validation phases.

Comparison of the ultimate bearing capacities of a square footing, predicted by ANN and simulation, by using the 70% training datasets, is shown in Figure 17. The coefficient of efficiency (R^2), demarcating the agreeability between the simulated and predicted values, is found to be 0.998 for training phase, which indicates a well-trained neural architecture. After the network is trained, the efficacy of the developed ANN model is checked by exposing it to the testing dataset for the prediction of the ultimate bearing capacity. The result of the testing phase is exhibited in Figure 18, as a comparison between the predicted and simulated q_u values. The simulated and predicted values are found to be in close agreement, the coefficient of efficiency (R^2) achieved in the testing phase being 0.996. This indicates that the developed ANN model is capable of predicting ultimate bearing capacity of foundation soil with highly acceptable accuracy.

Once the training phase of the model has been successfully accomplished, the performance of the trained model is subjected to the validation data, which have not been used as part of the model building process. The purpose of the model validation phase is to ensure that the model has the ability to generalize 'within the limits' set by the training data, rather than simply having memorized the input-output relationships embedded in the training data. The comparison of the target and predicted ultimate bearing capacities, obtained from the validation phase, is presented in Figure 19, and exhibits a high coefficient of efficiency (R^2) equal to 0.998.

6.2.3 Sensitivity analysis

Sensitivity analysis is of extreme importance for selection of influencing input variables. Different tactics have been suggested in the literature to identify the contributory input variables. Goh (1994) and Shahin, Maier, and Jaksa (2002) have used Garson's algorithm (1991), in which the input-hidden layer (Table 2) and hidden-output layer (Table 3) connection weights of the trained ANN model are partitioned, and the absolute values of the weights are taken to distinguish the important input variables (Eq. 3). The output from Garson's algorithm

provides the ranking of the parameters based on their relative importance. Hence, the ranking does not establish any direct or inverse correlation between the input variables and the output. These details have been exemplified by Goh (1994). Olden, Joy, and Death (2004) presented the connection weights approach, in which the actual product of the input-hidden and hidden-output connection weights are considered (Eq. 4). The result is a ranking of the input variables based on their magnitudes, while at the same time the absolute values provide the idea whether the outputs are having a direct or inverse relation with different input parameters (Table 4). Accordingly, the following expressions represent the estimation of variable importance for predictor variable X (where X = 1-7), using the weights connecting each of the input neurons Z (where Z = 1–7) to each of the hidden neurons N (where N = 1–10), and the latter to the single output neuron.

$$Input_X = \sum_{N=1}^{10} \frac{\left|Hidden_{XN}\right|}{\sum_{Z=1}^{7}\left|Hidden_{ZN}\right|} \quad \text{(Garson's algorithm)} \tag{3}$$

$$Input_X = \sum_{N=1}^{10} Hidden_{XN} \quad \text{(Connection weight approach)} \tag{4}$$

The sensitivity analysis for the developed ANN model, as per Garson's method (Das and Basudhar 2006; Shahin, Maier and Jaksa 2002; Das and Basudhar 2008) and the connection weight approach (Olden et al. 2004), to establish the importance ranking of the input parameters, are presented in Table 5 and Table 6. The angle of internal friction, φ has been found to be the most important input parameter followed by c, D_f/B, b/B, B, β and γ as per Garson's method, represented as pie-chart in Figure 20. It can also be seen that as per the connection weight approach, D_f/B is the most important input parameter followed by B, φ, b/B, c, β and γ. Hence, based on an overall understanding, the angle of internal friction of the constituent soil and the embedment depth are considered to be the most influencing on the ultimate bearing capacity of the footing resting on the crest of a c-φ slope.

7.0 CONCLUSIONS

Based on the present study, the following significant conclusions are established:

- Mesh convergence study defines an optimal mesh size for the PLAXIS 3D models so as to obtain accurate solutions from the numerical simulation.

- Bearing capacity of a footing, resting on the crest of the slope, increases with the increase in the shear strength parameters of constituent material, footing width and the embedment depth, while it reduces with the increase in the slope inclination.
- Bearing capacity increases with the increasing setback distance, and beyond a critical setback ratio $(b/B)_{critical} = 4$, the footing responds to a similar one resting on horizontal semi-infinite medium.
- The variation of unit weight of soil has negligible effect on the ultimate bearing capacity.
- The model with 10 numbers of neurons in the hidden layer proved to be the 'best' model for the 7-10-1 ANN architecture to obtain the ultimate bearing capacity.
- Based on sensitivity analyses as per Garson's algorithm and Connection-weight approaches, angle of internal friction, φ, and embedment depth ratio, D_f/B, are the most important input parameters for estimating the ultimate bearing capacity of square footing resting on crest sloping ground.

In the present context of growing urbanization in the hill-slopes, it is imperative to study the influence of planned or unplanned construction on altering the stability of the natural slopes. In this regard, the present study reports the outcome of a finite element based 3-D analysis carried out to study the behaviour and influence of a shallow square footing resting on a dry homogeneous c-φ soil slope. The primary aim of the study was to understand the evolution of failure mechanisms beneath such footings and their influence on the slope stability. In this regard, it is worth mentioning that the scope of the work reported herein is a simplified approach to the stated problem. Hill-slope urbanization consists of multiple adjacent footings of various shapes, sizes and embedment depths, which characteristically influence the stability. However, such combination of adjacent footings has not been addressed in this study. Moreover, the hill-slope in this study has been assumed to be of uniform geometry and comprising of perfectly dry and homogeneous soil characteristics. In the contrary, in-situ, the hill-slope would comprise of variations in soil properties, presence of water table, variation in field geometry and hill-slope geology, the influence of which has not been addressed in the present study. Hill-slope in the north-east India is often subjected to intense rainfall and intermittent seismic shaking, the effects of which are beyond the scope of the present study. In a nutshell, although there are several issues which are not addressed in the present study, yet the reports in the article about the evolution of the failure mechanism is immensely important to develop basic idea and apply it for different complexities as described above.

385 **References**

386 Acharyya, R., and A. Dey. 2017. "Finite element investigation of the bearing capacity of square footings resting
387 on sloping ground." *INAE Letters* 2 (3): 97-105.

388 Azzam, W. R., and A. Farouk. 2010. "Experimental and numerical studies of sand slopes loaded with skirted
389 strip footing." *Electronic Journal of Geotechnical Engineering* 15 (H): 795-812.

390 Azzam, W. R., and A. Z. El-Wakil. 2015. "Experimental and numerical studies of circular footing resting on
391 confined granular subgrade adjacent to slope." *International Journal of Geomechanics, ASCE* 16 (1) 1-15.

392 Bauer, G. E., D. H. Shields, J. D. Scott, and J. E. Gruspier. 1981. "Bearing capacity of footing in granular
393 slope." *Proceedings of 11th International Conference on Soil Mechanics and Foundation Engineering*,
394 Balkema, Rotterdam, The Netherlands, 2: 33-36.

395 Behera, R. N., C. R. Patra, N. Sivakugan, and B. M. Das. 2013. "Prediction of ultimate bearing capacity of
396 eccentrically inclined loaded strip footing by ANN: Part I.", *International Journal of Geotechnical*
397 *Engineering* 7 (1): 36-44.

398 Behera, R. N., C. R. Patra, N. Sivakugan, and B. M. Das. 2013. "Prediction of ultimate bearing capacity of
399 eccentrically inclined loaded strip footing by ANN.": part II, *International Journal of Geotechnical*
400 *Engineering* 7 (2): 165-172.

401 Castelli, F., and V. Lentini. 2012. "Evaluation of the bearing capacity of footings on slopes." *International*
402 *Journal of Physical Modelling in Geotechnics* 12 (3): 112-118.

403 Cerato, A. B., and A. J. Lutenegger. 2006. "Bearing capacity of square and circular footings on a finite layer of
404 granular soil underlain by a rigid base." *Journal of Geotechnical and Geoenvironmental Engineering* 132
405 (11): 1496-1501.

406 Cerato, A. B., and A. J. Lutenegger. 2007. "Scale effects of shallow foundation bearing capacity on granular
407 material." *Journal of Geotechnical and Geoenvironmental Engineering* 133 (10): 1192-1202.

408 Das S. K., and P. K. Basudhar. 2008. "Prediction of residual friction angle of clay using artificial neural
409 network." *Engineering Geology* 100: 142-145.

410 Das, S. K., and P. K. Basudhar. 2006. "Undrained lateral load capacity of piles in clay using artificial neural
411 network." *Computers and Geotechnics* 33: 454-459.

412 Das, S. K., P. Samui., A. K. Sabat, and T. G. Sitharam. 2010. "Prediction of swelling pressure of soil using
413 artificial intelligence technique." *Environmental Earth Science* 61: 393-403.

414 Das, S. K., P. Samui, and A. K. Sabat. 2012. “Prediction of field hydraulic conductivity of clay liners using an
415 artificial neural network and support vector machine.” *International Journal of Geomechanics, ASCE* 12:
416 606-611.
417 Hagan, M. T., H. B. Demuth, and M. Beale. 1996. “*Neural Network Design”*, PWS Publishing Company,
418 Boston, USA.
419 Drescher, A., and E. Detournay. 1993. “Limit load in translational failure mechanisms for associative and non-
420 associative materials.” *Geotechnique* 43 (3): 443-456.
421 Erzin, Y., S. D. Gumaste, A. K. Gupta, and D. N. Singh. 2009. “Artificial neural network (ANN) models for
422 determining hydraulic conductivity of compacted fine-grained soils.” *Canadian Geotechnical Journal* 46:
423 955-968.
424 Garson, G. D. 1991. “Interpreting neural-network connection weights.” *Artificial Intelligence Expert* 6 (7): 47-
425 51.
426 Ghaboussi, J., D. E. Sidarta, and P. V. Lade. 1994. “Neural network based modelling in geomechanics.”
427 *Computer Methods and Advances in Geomechanics*, Balkema, Rotterdam Publishing 153-164.
428 Goh, A. T. C. 1994. “Seismic liquefaction potential assessed by neural networks.” *Journal of Geotechnical and*
429 *Geoenvironmental Engineering* 120 (9): 1467-1480.
430 Hansen, J. B. 1970. “A revised and extended formula for bearing capacity.” Danish Geotechnical Institute,
431 Bulletin 28: 5-11.
432 Hebb, D. O. 2002. “*The Organization of Behaviour: A Neurophysiological Approach*” Lawrence Erlbaum
433 Publishers, Associates, Mahwah, New Jersey.
434 Keskin, M. S., and M. Laman. 2013. “Model studies of bearing capacity of strip footing on sand slope.” *KSCE*
435 *Journal of Civil Engineering* 17 (4): 699-711.
436 Kumar, S. V. A., and K. Ilamparuthi. 2009. “Response of footing on sand slopes.” In: Indian Geotechnical
437 Conference, Guntur, India, 622–626.
438 Kuo, Y. L., M. B. Jaksa, A. V. Lyamin, and W. S. Kaggwa. 2009. “ANN-based model for predicting the bearing
439 capacity of strip footing on multi-layered cohesive soil.” *Computers and Geotechnics* 36: 503-516.
440 Lavasan, A. A., and M. Ghazavi. 2014. “Failure mechanism and soil deformation pattern of soil beneath
441 interfering square footings.” *Numerical Methods in Civil Engineering* 1 (2): 48-56.
442 Lee, M. I., and H. J. Lee. 1996. “Prediction of pile bearing capacity using neural networks.” *Computers and*
443 *Geotechnics* 18 (3): 189-200.

444 MathWorks. 2001. "*Matlab user's manual*" Version 2015A, The MathWorks, Inc., Natick.

445 McCulloch, W. S., and W. Pitts. 1943. "A logical calculus in the ideas immanent in nervous activity.", *Bulletin*
446 *of Mathematical Biophysics* 5: 115-133.

447 Meyerhof, G. G. 1951. "The ultimate bearing capacity of foundations." *Geotechnique* 2: 301-332.

448 Mishra, A. K., B. Kumar, and J. Dutta. 2016. "Prediction of hydraulic conductivity of soil bentonite mixture
449 using hybrid-ANN approach." *Journal of Environmental Informatics* 27 (2): 98-105.

450 Momeni, E., R. Nazir, D. J. Armaghani, and H. Maizir. 2014. "Prediction of pile bearing capacity using a hybrid
451 genetic algorithm-based ANN." *Measurement* 57: 122-131.

452 Nasr, A. M. 2014. "Behaviour of strip footing on fiber-reinforced cemented sand adjacent to sheet pile wall."
453 *Geotextiles and Geomembranes* 42: 599-610.

454 NDMA. 2013. Catalogue of Building Typologies in India: Seismic vulnerability assessment of building types in
455 India, A report submitted by the Seismic Vulnerability Project Group of IIT Bombay, IIT Guwahati, IIT
456 Kharagpur, IIT Madras and IIT Roorkee to the National Disaster Management Authority, India.

457 Noorzaei, J., S. J. S. Hakim, and M. S. Jaafar. 2008. "An approach to predict ultimate bearing capacity of
458 surface footings using artificial neural network." *Indian Geotechnical Journal* 38 (4): 513-526.

459 Olden J. D., M. K. Joy, and R. G. Death. 2004. "An accurate comparison of methods for quantifying variable
460 importance in artificial neural networks using simulated data." *Ecological Modelling* 178(3): 389-397.

461 Rosenblatt, F. 1958. "The perception: a probabilistic model for information storage and organization in brain."
462 *Psychological Review* 68: 368-408.

463 Shahin, M. A., H. R. Maier, and M. B. Jaksa. 2002. "Predicting settlement of shallow foundations using neural
464 networks." *Journal of Geotechnical and Geoenvironmental Engineering ASCE* 128 (9): 785-793.

465 Shields, D. H., J. D. Scott, G. E. Bauer, J. H. Deschenes, and A. K. Barsvary. 1977. "Bearing capacity of
466 foundation near slopes." *Proceedings of the 10th International Conference on Soil Mechanics and*
467 *Foundation Engineering Japanese Society of Soil Mechanics and Foundation Engineering*, Tokyo, Japan, 1:
468 715-720.

469 Shukla, R. P., and R. S. Jakka. 2017. "Discussion on Experimental and numerical studies of circular footing
470 resting on confined granular subgrade adjacent to slope by WR Azzam and AZ El-Wakil." *International*
471 *Journal of Geomechanics ASCE* 17 (2): 1-3.

472 Terzaghi, K. 1943. "*Theoretical Soil Mechanics*" John Wiley and Sons Inc., New York, USA.

Vesic, A. S. 1973. "Analysis of ultimate loads of shallow foundation." *Journal of Soil Mechanics Found Division ASCE* 99 (SM1): 45-73.

Xiao-Li, Y., G. Nai-Zheng, Z. Lian-Heng, and Z. Jin-Feng. 2007. "Influences of non-associated flow rules on seismic bearing capacity factors of strip footing on soil slope by energy dissipation method." *Journal of Central South University of Technology* 14 (842).

Yu, L., J. Liu, X. J. Kong, and Y. Hu. 2010. "Three-dimensional large deformation FE analysis of square footings in two-layered clays." *Journal of Geotechnical and Geoenvironmental Engineering ASCE* 137 (1): 52-58.

Zhu, M., and R. L. Michalowski. 2005. "Shape factors for limit loads on square and rectangular footings." *Journal of Geotechnical and Geoenvironmental Engineering* 131 (2): 223-231.

Table 1 Properties of concrete used for modelling the strip footing

Unit weight (γ) (kN/m^3)	Modulus of elasticity E (GPa)	Poisson's ratio (ν)
25	22	0.15

Table 2 Input-Hidden layer connection weights obtained after training phase

N / X	Hidden N1	Hidden N2	Hidden N3	Hidden N4	Hidden N5	Hidden N6	Hidden N7	Hidden N8	Hidden N9	Hidden N10
c (X1)	0.55	-0.67	-0.26	0.84	-0.54	0.95	0.58	-3.58	0.004	-0.12
φ (X2)	-0.56	-0.33	8.43	1.30	-0.64	-7.25	1.27	-5.25	-0.29	-0.91
γ (X3)	0.32	0.03	0.02	0.16	-0.09	0.03	0.09	-0.75	-0.01	0.04
B (X4)	0.24	0.11	0.15	0.46	-0.52	-0.06	0.46	4.79	-0.13	-0.13
b/B (X5)	1.45	0.0008	2.05	0.14	0.07	-1.74	-0.51	2.64	0.02	2.01
B (X6)	-0.38	-0.01	-0.47	-0.04	-0.01	0.51	0.11	-0.67	0.004	-0.46
D_f/B (X7)	1.30	0.57	-0.66	0.72	-0.35	0.66	0.42	6.50	-0.09	-0.05

Table 3 Hidden-Output layer connection weights obtained after training phase

N / **Y**	Hidden N1	Hidden N2	Hidden N3	Hidden N4	Hidden N5	Hidden N6	Hidden N7	Hidden N8	Hidden N9	Hidden N10
Output	0.06	-2.16	0.52	1.91	2.01	0.53	0.83	2.32	-3.58	0.97

514 Table 4 Product of the input-hidden and hidden-output connection weights

N / X	Hidden N1	Hidden N2	Hidden N3	Hidden N4	Hidden N5	Hidden N6	Hidden N7	Hidden N8	Hidden N9	Hidden N10
c (X1)	0.04	1.45	-0.13	1.61	-1.09	0.50	0.48	-8.31	0.02	-0.12
φ (X2)	-0.04	0.71	4.40	2.49	-1.29	-3.83	1.06	-12.18	1.03	-0.88
γ (X3)	0.02	-0.07	0.01	0.31	-0.19	0.02	0.08	-1.73	0.02	0.04
B (X4)	0.02	-0.24	0.08	0.87	-1.04	-0.03	0.38	11.10	0.48	-0.12
b/B (X5)	0.09	0.0018	1.07	0.26	0.14	-0.92	-0.43	6.13	-0.07	1.94
B (X6)	-0.02	0.03	-0.24	-0.08	-0.01	0.27	0.09	-1.55	0.01	-0.45
D_f/B (X7)	0.08	-1.23	-0.34	1.37	-0.69	0.35	0.35	15.09	0.32	-0.05

515

516

517 Table 5 Importance ranking of input-parameters based on Garson's algorithm

Input	Relative importance	Relative importance (%)	Rank
c	1.69	18.07	2
φ	3.54	37.80	1
γ	0.19	2.02	7
B	1.05	11.24	5
b/B	1.23	13.12	4
β	0.30	3.18	6
D_f/B	1.36	14.57	3

518

519 Table 6 Importance ranking of input-parameters based on Connection weight approach

Input	Relative importance	Rank
c	-5.57	5
φ	-8.54	3
γ	-1.50	7
B	11.50	2
b/B	8.21	4
β	-1.97	6
D_f/B	15.25	1

520

521

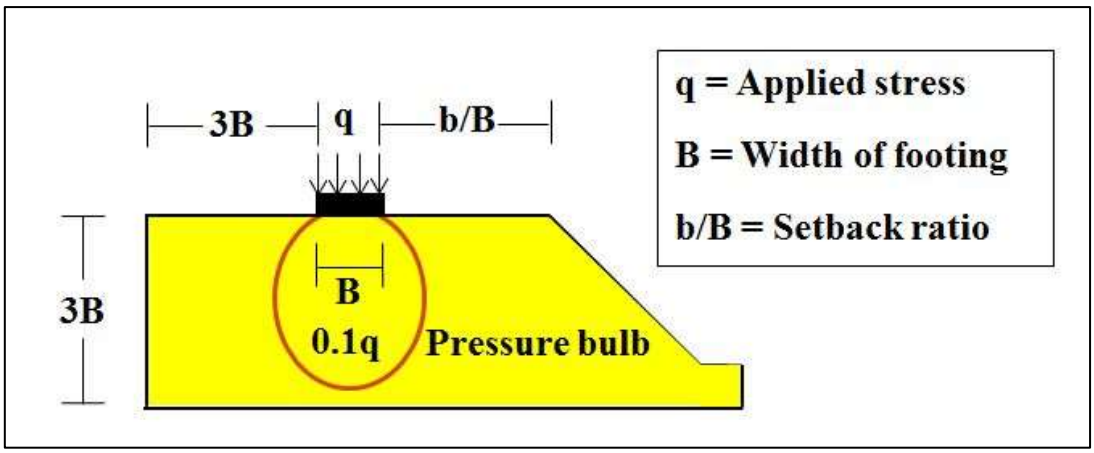

522

523 Figure 1 Schematic representation of a footing resting on crest of a sloping ground (not to scale)

524

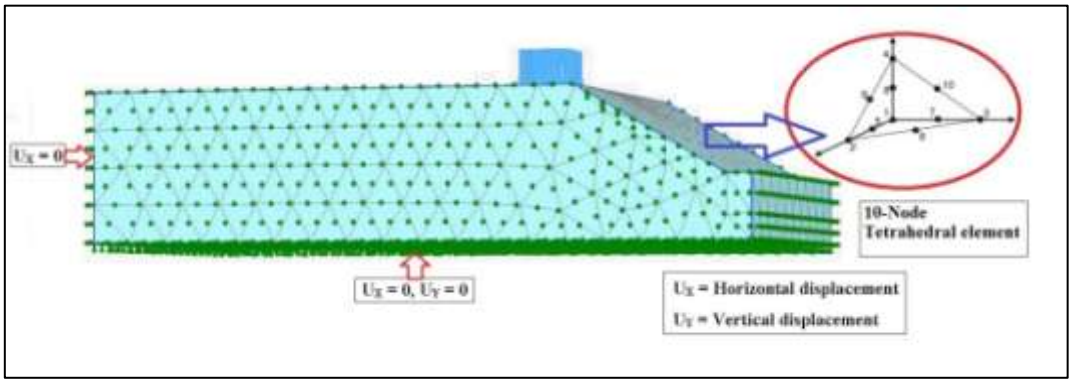

525

526 Figure 2 Typical meshing scheme and application of standard fixities in the numerical model

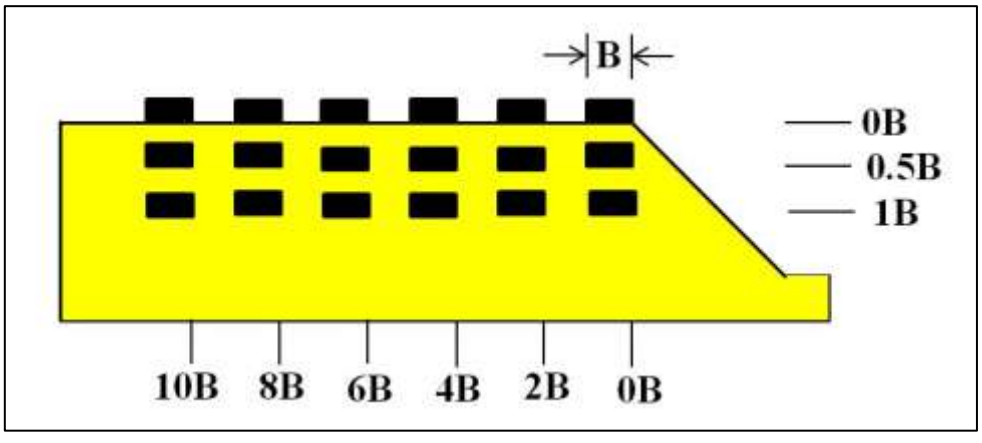

527

528 Figure 3 Locations of surface and embedded footings in the crest of a sloping ground

529

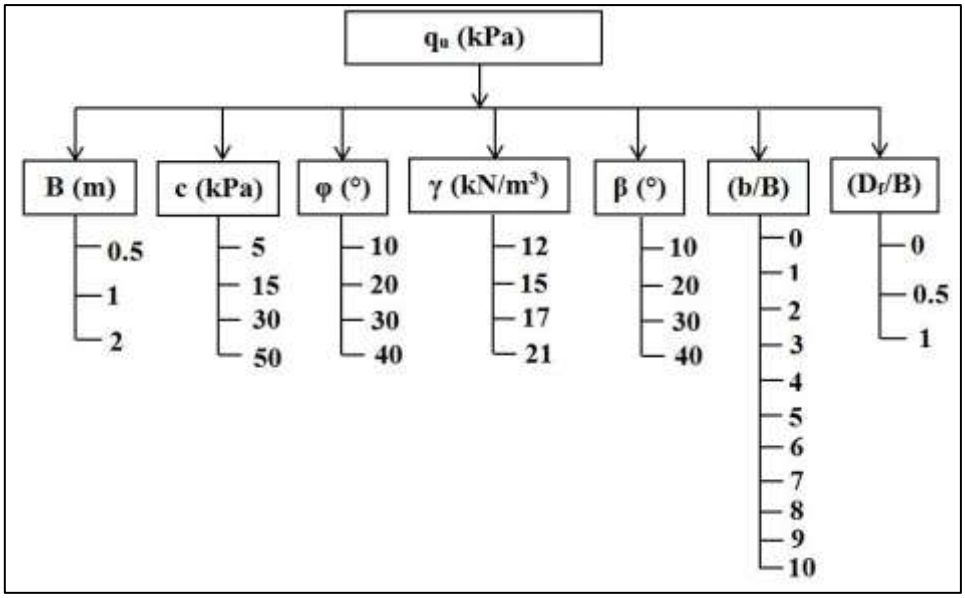

530

531 Figure 4 Geotechnical and geometrical parameters considered in the present study

532

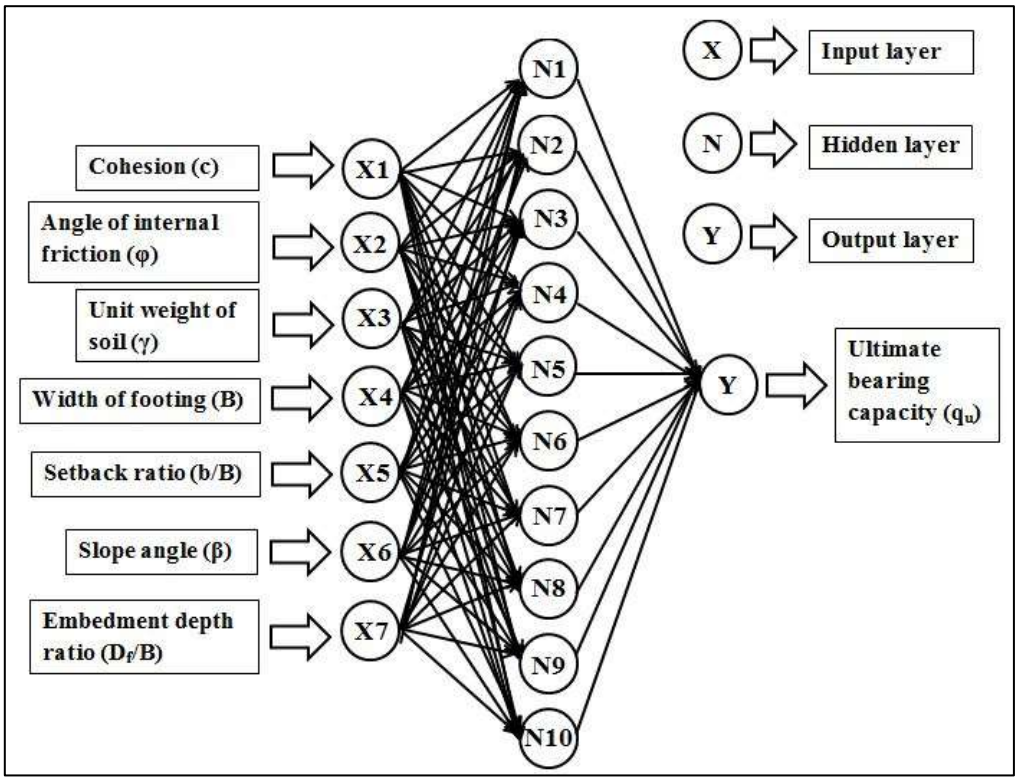

533

534 Figure 5 Artificial neural network architecture used in the present study

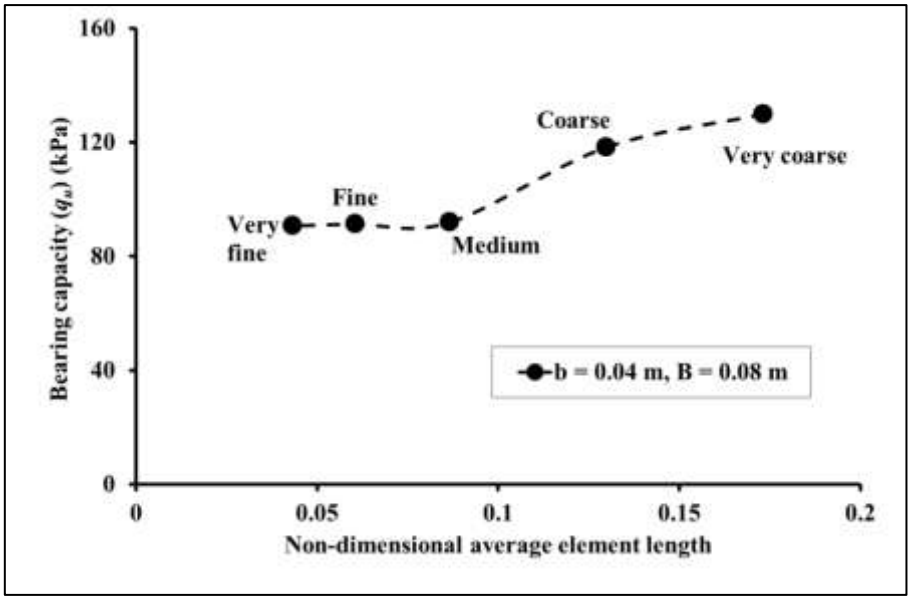

535

536 Figure 6 Convergence study for determining the optimum mesh size for FE analysis

537

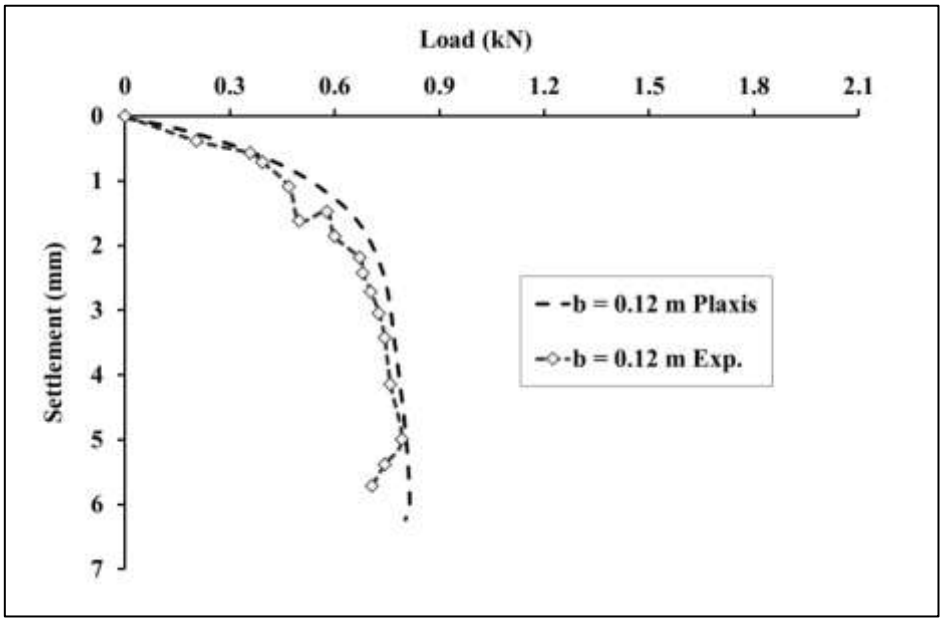

538

539 Figure 7 Validation of the numerical model with experimental investigation by Castelli and Lentini (2012)

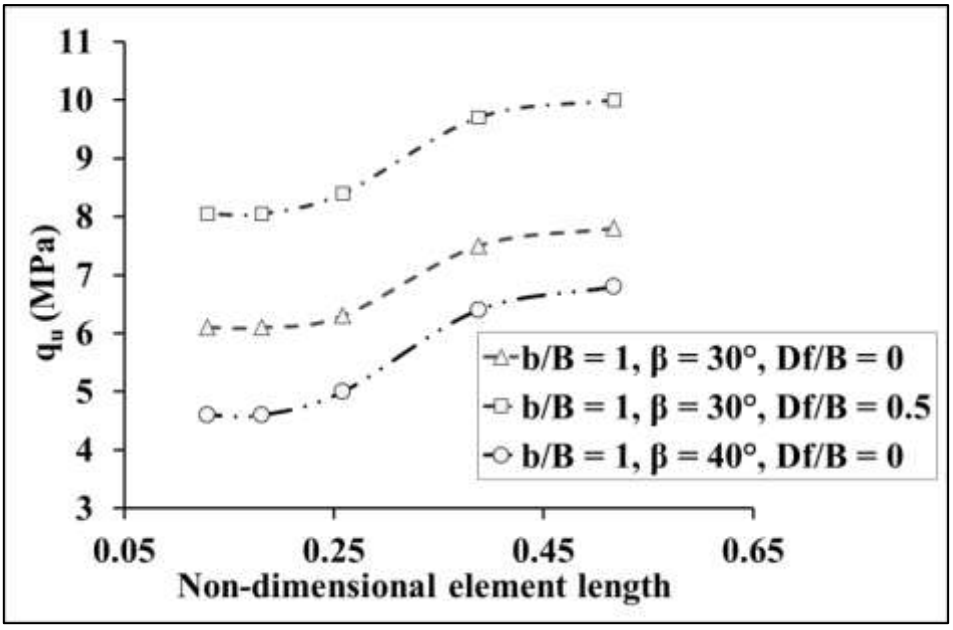

Figure 8 Typical convergence study for footing resting on sloping ground

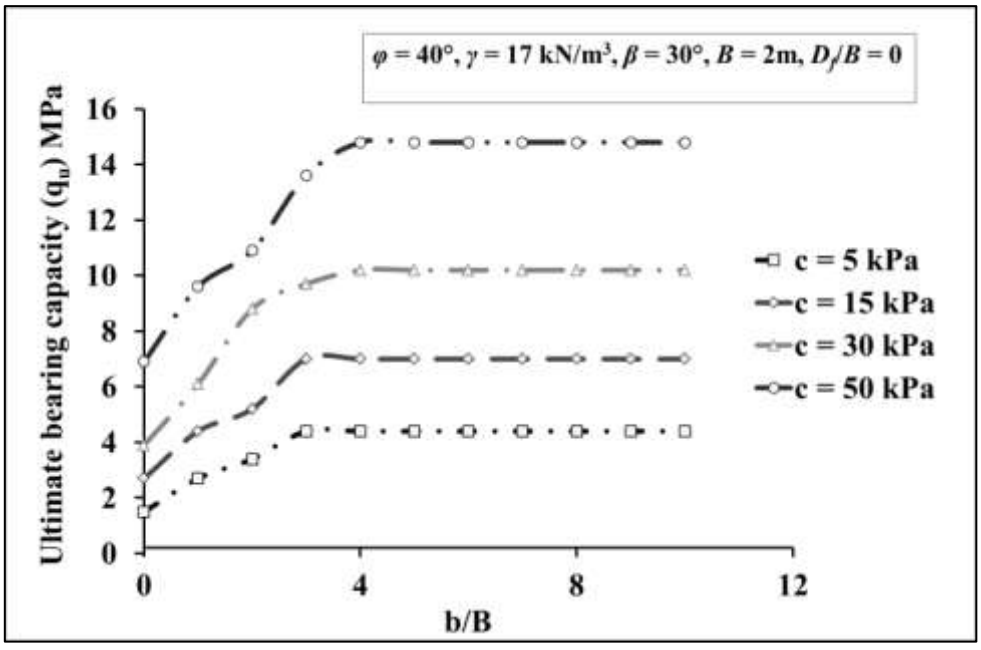

Figure 9 Typical variation of q_u with cohesion (c) and setback ratio (b/B)

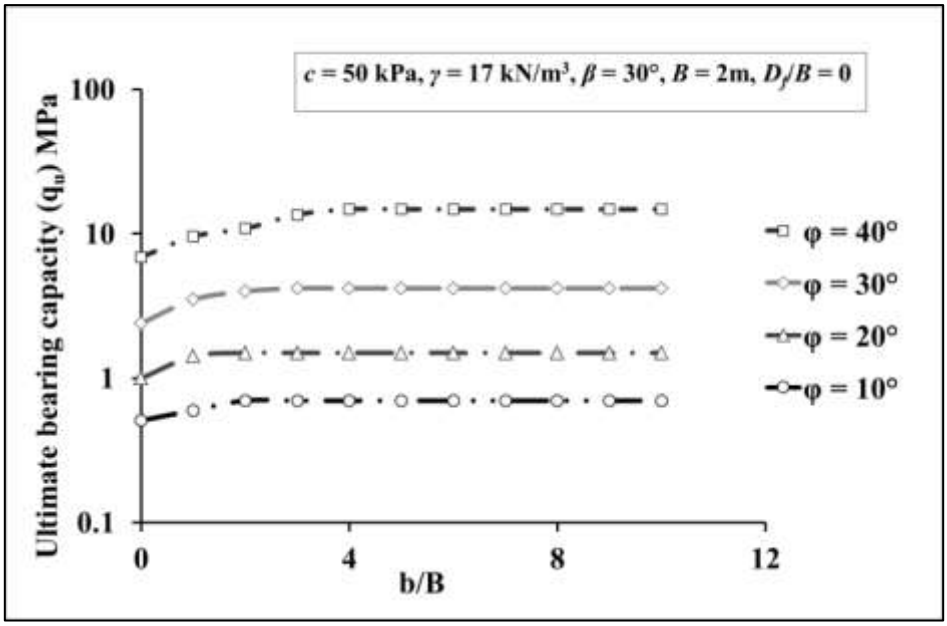

545

546 Figure 10 Typical variation of q_u with angle of internal friction (φ) and setback ratio (b/B)

547

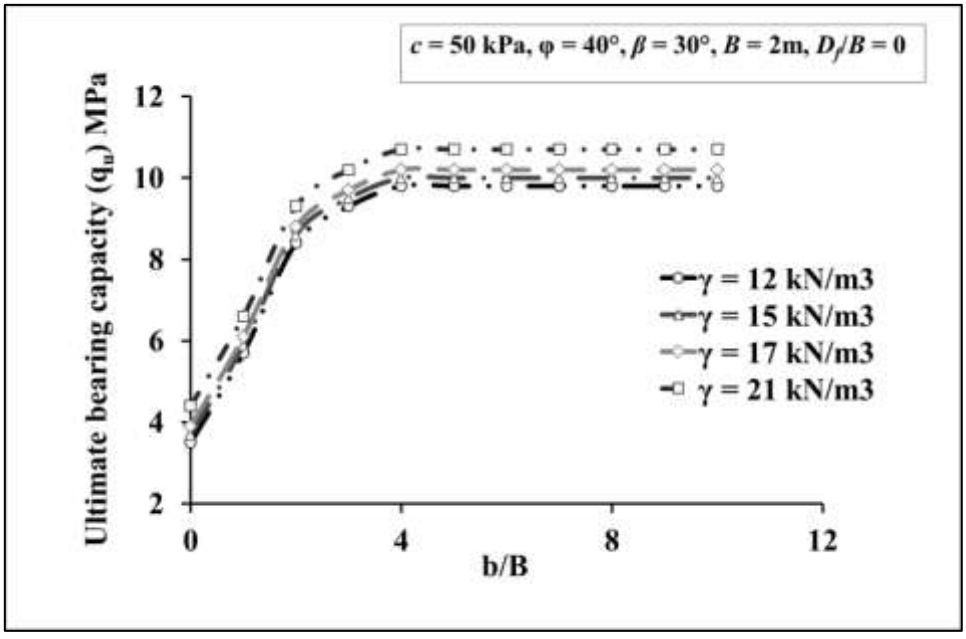

548

549 Figure 11 Typical variation of q_u with unit weight of soil (γ) and setback ratio (b/B)

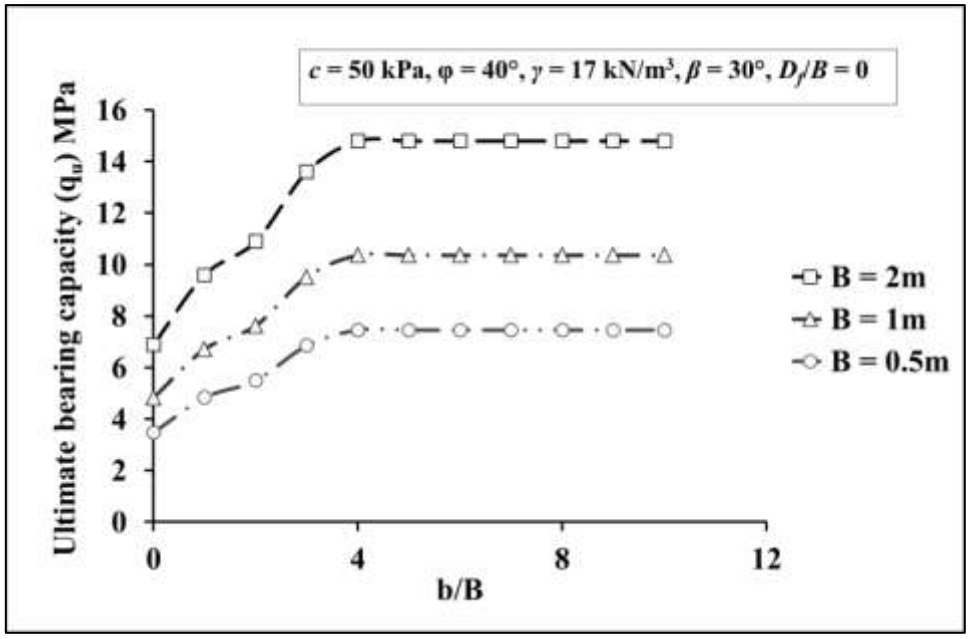

Figure 12 Typical variation of q_u with footing width (B) and setback ratio (b/B)

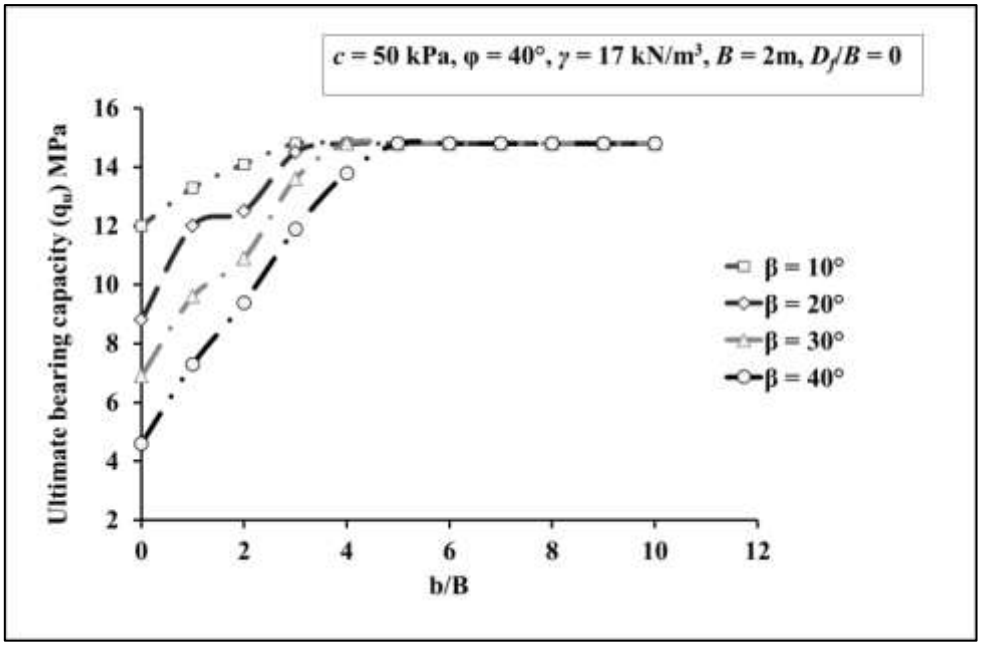

Figure 13 Typical variation of q_u with slope angle (β) and setback ratio (b/B)

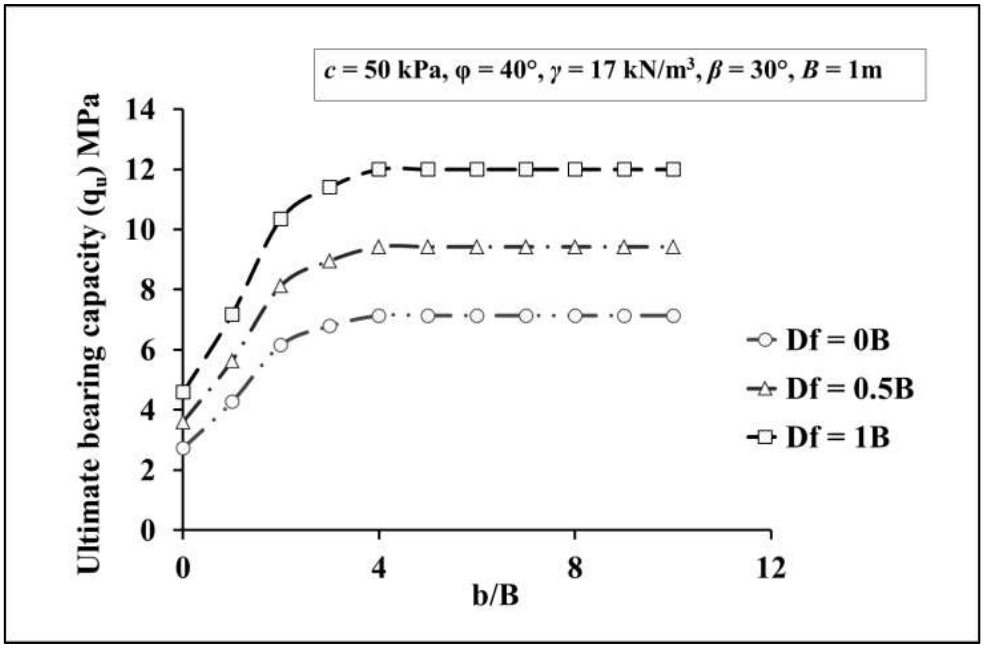

555

556 Figure 14 Typical variation of q_u with unit weight of soil (D_f/B) and setback ratio (b/B)

557

558

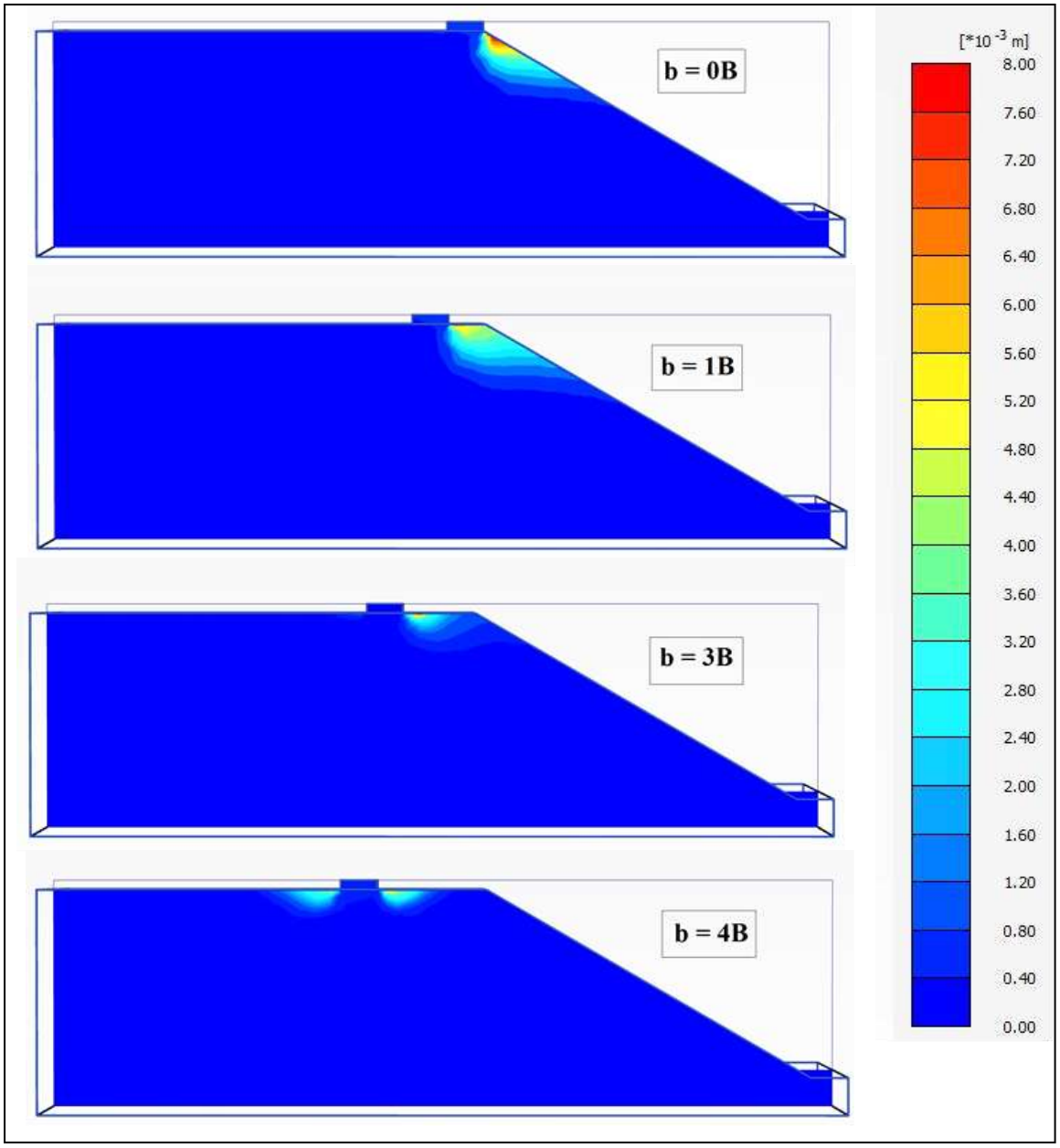

559

560 Figure 15 Typical formations of passive zones beneath the footing for various setback ratios (*b/B*)

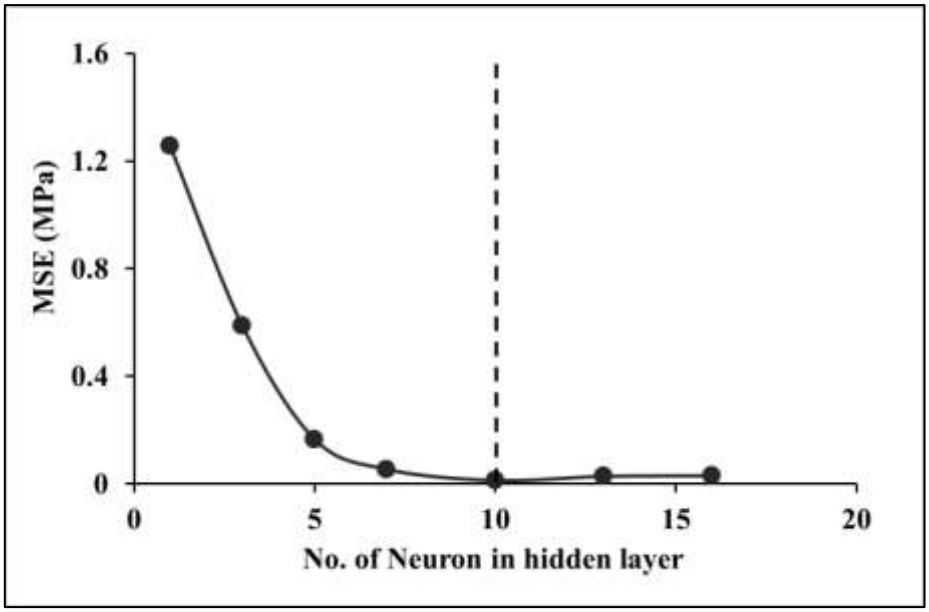

561

562 Figure 16 Determination of optimum number of neurons in the hidden layer

563

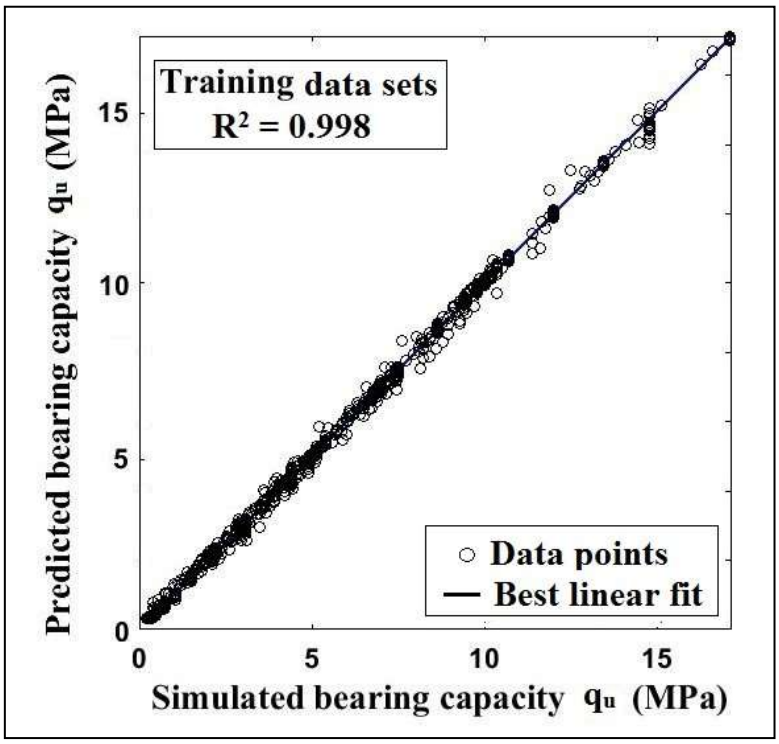

564

565 Figure 17 Performance of artificial neural network model during training phase

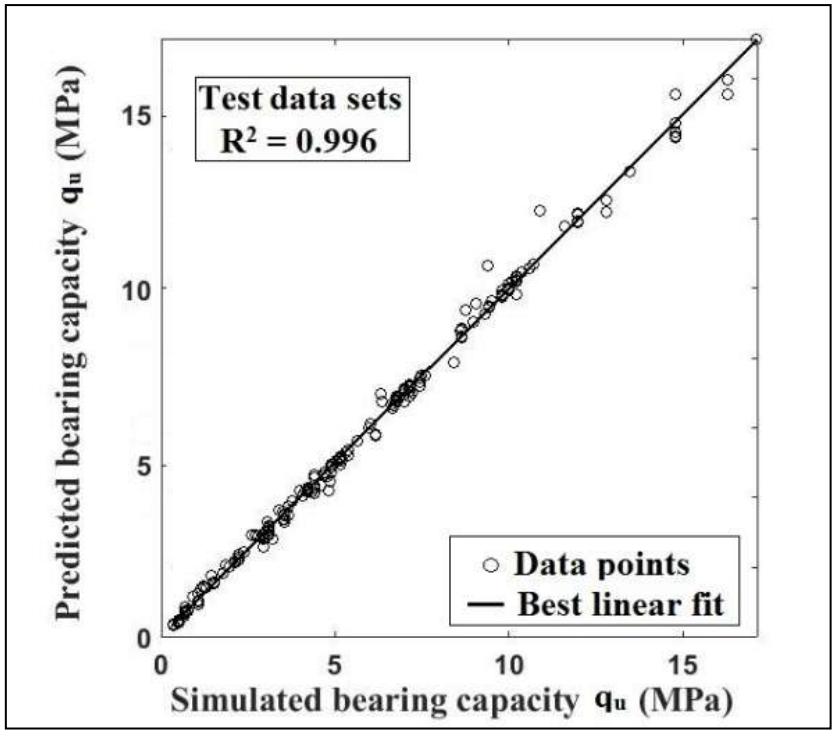

566

567 Figure 18 Performance of artificial neural network model during testing phase

568

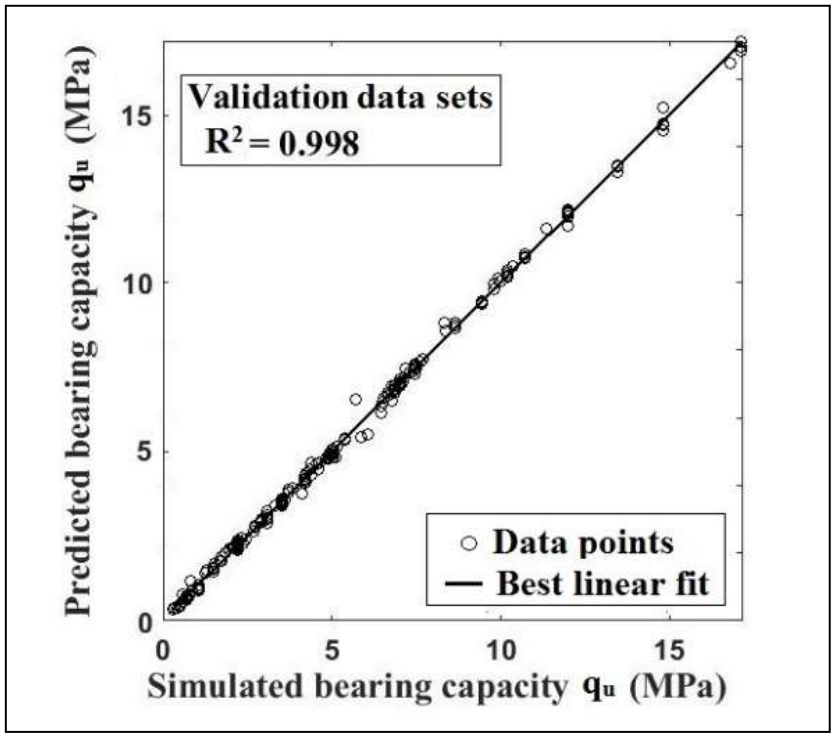

569

570 Figure 19 Performance of artificial neural network model for validation phase

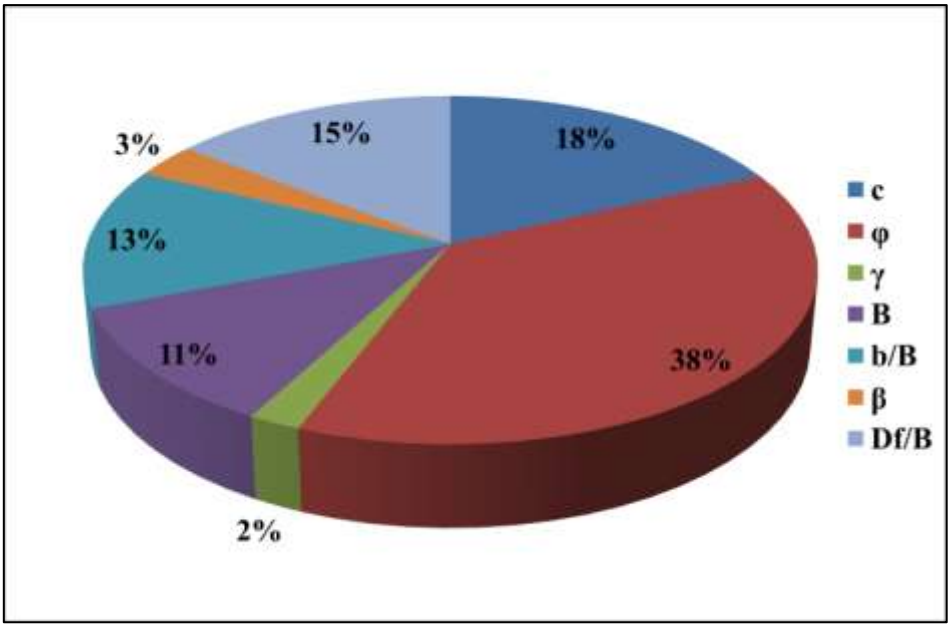

Figure 20 Relative importances of the parameters according to Garson's algorithm (1991)